J. Am. Soc. Mass Spectrom. (2019) 30:256–267
DOI: 10.1007/s13361-018-2074-z

RESEARCH ARTICLE

Conditions for Analysis of Native Protein Structures Using Uniform Field Drift Tube Ion Mobility Mass Spectrometry and Characterization of Stable Calibrants for TWIM-MS

Julian A. Harrison,[1,2] Celine Kelso,[1,2] Tara L. Pukala,[3] Jennifer L. Beck[1,2]

[1]School of Chemistry, University of Wollongong, Wollongong, NSW 2522, Australia
[2]Molecular Horizons, University of Wollongong, Wollongong, NSW 2522, Australia
[3]Discipline of Chemistry, University of Adelaide, Adelaide, SA 5005, Australia

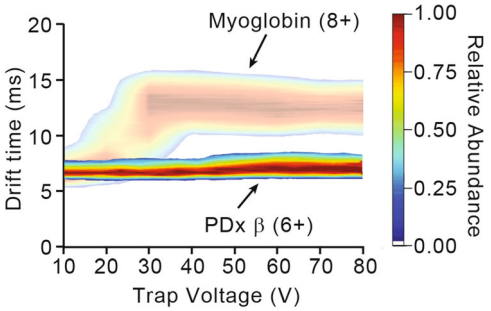

Abstract. Determination of collisional cross sections (CCS) by travelling wave ion mobility mass spectrometry (TWIM-MS) requires calibration against standards for which the CCS has been measured previously by drift tube ion mobility mass spectrometry (DTIM-MS). The different extents of collisional activation in TWIM-MS and DTIM-MS can give rise to discrepancies in the CCS of calibrants across the two platforms. Furthermore, the conditions required to ionize and transmit large, folded proteins and assemblies may variably affect the structure of the calibrants and analytes. Stable heterooligomeric phospholipase A_2 (PDx) and its subunits were characterized as calibrants for TWIM-MS. Conditions for acquisition of native-like TWIM (Synapt G1 HDMS) and DTIM (Agilent 6560 IM-Q-TOF) mass spectra were optimized to ensure the spectra exhibited similar charge state distributions. CCS measurements (DTIM-MS) for ubiquitin, cytochrome *c*, holo-myoglobin, serum albumin and glutamate dehydrogenase were in good agreement with other recent results determined using this and other DTIM-MS instruments. PDx and its β and γ subunits were stable across a wide range of cone and trap voltages in TWIM-MS and were stable in the presence of organic solvents. The CCS of PDx and its subunits were determined by DTIM-MS and were used as calibrants in determination of CCS of native-like cytochrome *c*, holo-myoglobin, carbonic anhydrase, serum albumin and haemoglobin in TWIM-MS. The CCS values were in good agreement with those measured by DTIM-MS where available. These experiments demonstrate conditions for analysis of native-like proteins using a commercially available DTIM-MS instrument, characterize robust calibrants for TWIM-MS, and present CCS values determined by DTIM-MS and TWIM-MS for native proteins to add to the current literature database.

Keywords: Native mass spectrometry, Drift tube ion mobility mass spectrometry, Travelling wave ion mobility mass spectrometry

Abbreviations DTIM-MS Drift tube ion mobility mass spectrometry; ESI Electrospray ionization; ESI-MS Electrospray ionization mass spectrometry; GDH Glutamate dehydrogenase; HSA Human serum albumin; IMMS Ion mobility mass spectrometry; PDx Phospholipase A_2/paradoxin from *Oxyuranus microlepidotus*; TWIM-MS Travelling wave ion mobility mass spectrometry

Received: 5 August 2018/Revised: 14 September 2018/Accepted: 20 September 2018/Published Online: 15 October 2018

Julian A. Harrison and Celine Kelso contributed equally to this work.

Senior authors Tara L. Pukala and Jennifer L. Beck contributed equally to this work.

Electronic supplementary material The online version of this article (https://doi.org/10.1007/s13361-018-2074-z) contains supplementary material, which is available to authorized users.

Correspondence to: Jennifer Beck; *e-mail:* jbeck@uow.edu.au

Introduction

Electrospray ionization mass spectrometry (ESI-MS) has been applied for more than 20 years to the analysis of non-covalent biomolecular complexes [1]. These studies can be applied to determine properties such as the relative strengths

of binding interactions, the quaternary structure of protein complexes and screening for ligand (such as drug molecules)-biomolecule interactions. A nuanced understanding of the solution and gas phase conditions that maintain a native or native-like (folded) structure is critical to ensuring the relevance of these analyses. In recent times, the coupling of (nano)ESI-MS with ion mobility mass spectrometry (IMMS) has offered the promise of adding to the structural information available from ESI-MS alone. IMMS can provide measurements of collisional cross section (CCS) and can also be used to compare the conformations and unfolding of biomolecules [2] and biomolecular complexes under different conditions [3], and to characterize the quaternary structure of protein complexes [4].

The most widely applied form of ion mobility analysis uses a drift tube and is readily coupled with mass spectrometry (drift tube ion mobility mass spectrometry, DTIM-MS, [5, 6]). In this ion mobility technique, ions in a drift tube experience a static uniform electric field. The tube has traditionally been filled with helium as the drift gas, and the ions are propelled in the direction of the applied field. The mobility of an ion (K_o, at standard temperature and pressure) and its associated drift time is related to its CCS (Ω), which can be calculated using the Mason-Schamp equation (described in [7]). The analysis of larger biomolecules by ESI-IMMS has become more accessible with the commercial availability of travelling wave ion mobility (TWIM) in which the mobility cell consists of a stacked ring ion guide to which a dynamic voltage wave is applied. Ions of higher mobility travel with the wave, while those of lower mobility roll over the wave and take longer to traverse the mobility cell that contains a gas (usually nitrogen) [8, 9]. This mobility cell has been coupled with a quadrupole time-of-flight (Q-TOF) mass spectrometer (Waters Synapt HDMS) allowing collision-induced dissociation (CID) products to be analysed by IMMS, and also the analysis of higher mass biomolecules (for reviews see [7, 10]). A drawback of this method is that owing to the changing electric field, the direct relationship between Ω and K_o no longer exists, and the TWIM-MS instrument must be calibrated using standards of known CCS, usually as determined using DTIM-MS [11–17]. One of the challenges in using calibrants of known CCS is that most CCS measurements were carried out by DTIM-MS using helium, while most TWIM-MS analyses are carried out in nitrogen. Recently, a commercial DTIM-MS instrument (Agilent 6560 IM-Q-TOF) in which the ion mobility cell is bracketed with ion funnels increasing sensitivity, and using nitrogen as the drift gas, has been developed. May et al. used this instrument to measure CCS in nitrogen for different classes of biomolecules and quaternary ammonium salts [18]. Stow et al. [16] have recently demonstrated that a CCS RSD (% relative standard deviation) of 0.29% was achievable across four laboratories using this instrument for a wide range of molecular types, masses and charge states. This instrument has a relatively high mass range (up to *m/z* 10,000). The commercial availability of this DTIM-MS provides opportunities to readily compare CCS determined by DTIM-MS and TWIM-MS.

Commonly used calibrants for determination of protein CCS using TWIM-MS are ubiquitin, cytochrome *c* and myoglobin [19, 20]. These proteins have been widely used because they were among the first proteins subjected to IMMS (especially DTIM-MS): they are readily commercially available, inexpensive, easy to handle, small and soluble in aqueous solution. Typically, ESI-MS analysis of proteins was carried out under denaturing solution conditions (in the presence of organic solvents and acidic conditions) that assist the ESI process; hence, early CCS measurements using DTIM-MS were typically of denatured proteins. Since these proteins were unfolded, they had relatively longer drift times, and could be considered as calibrants for higher mass, folded (native-like) proteins or protein complexes. The question as to whether denatured protein calibrants of known CCS (determined by DTIM-MS) should be used to calculate CCS of folded (native-like) biomolecules analysed using TWIM-MS has been the subject of investigation. IMMS determines rotationally averaged cross sections, and drift time is dependent on the number of collisions with the gas, the interaction potential with the charged analyte, the strength of the electric field and the charge(s) of the analyte [21]. Consideration of these variables is important in determining the best calibrants for a particular analyte. Salbo et al. [22] determined that native-like calibrant proteins of similar drift time and mass to the analyte protein should be used in TWIM-MS CCS calculations. Later, Robinson and co-workers [23] showed that selection of calibrants based simply on mass leads to greater error for proteins of unusual charge, such as for native-like membrane proteins which display relatively low charge for their mass compared with soluble proteins.

Taking these observations into account, calibrants and analytes with similar charge distribution on their surfaces and similar drift times will likely give the best experimental results. Konermann and co-workers [24] highlighted that calibrant and analyte ions must be analysed under the same conditions for determination of CCS by TWIM-MS, which must also be similar to those conditions used for the initial measurement of CCS of the calibrants by DTIM-MS. These conditions are difficult to satisfy, especially when determining the CCS of native-like proteins and protein complexes, because if the conditions are too soft (to maintain native folds) there may be problems with desolvation and transmission; if the conditions are too harsh, the protein of interest will unfold and native-like calibrants may be more or less sensitive to the conditions than the analyte. In addition, the different platforms for TWIM-MS and DTIM-MS mean that it can be experimentally challenging to arrive at conditions where the DTIM-MS conditions for measuring calibrant CCS match those in TWIM-MS. For example, Morsa et al. [25] have demonstrated that ions can be susceptible to heating in the high intensity electrical fields of TWIM-MS. Previously, Bush et al. [11] used a commercial Synapt HDMS instrument in which the TWIM cell was replaced by a drift cell with RF ion confinement in order to be able to directly measure CCS of ions of larger mass proteins and protein assemblies (high *m/z*), in helium and in nitrogen.

The commonly used calibrant proteins (ubiquitin, cytochrome *c* and myoglobin) readily unfold, and even in experienced hands under what are supposed to be native-like conditions, calibrant solutions may contain different populations of variably folded structures, and further unfolding may occur in the IM sector. This contributes to poorer resolution of drift times for different conformational forms, especially in TWIM-MS. For this reason, Konermann and co-workers recommended that intentionally denatured proteins should be used as calibrants even when native structures of proteins/complexes of interest are under investigation [23]. In addition, a number of reports have suggested that the best choices of molecules as calibrants should have similar physical and chemical properties to those under study [23, 26].

In view of the considerations above, an ideal calibrant for investigation of protein structures and conformations would be highly stable proteins which do not readily unfold, and that are capable of forming oligomers with charge distributions on their surfaces similar to the analyte. The formation of stable oligomers allows for detection of a range of charge states over a wider *m/z* range in the mass spectra, from lower *m/z* for monomers, to higher *m/z* for the oligomers. Examples of such proteins are the phospholipase A_2 (PLA_2) proteins from Australian and other snake venoms. Group I and II PLA_2 contain seven to eight disulfide bonds making them highly stable proteins that are resistant to unfolding by chemical denaturants and heat [27–29]. Taipan (e.g. *Oxyuranus microlepidotus*) venom PLA_2 (also known as paradoxin, PDx) forms trimers comprised of α, β and γ subunits [30]. These complexes are held together by salt bridges and hydrophobic interactions. Venom is regularly collected from Australian snakes for the production of anti-venom and PLA_2 proteins are readily purified by size exclusion chromatography. The stability of the PLA_2 proteins, their accessibility, ease of purification and the observation that a range of ions of different size and charge are evident in their mass spectra make PLA_2 useful as potential calibrants for IMMS analysis of proteins and protein assemblies.

In the current work, DTIM-MS instrument parameters were optimized for analysis of native protein structures, including the hexameric glutamate dehydrogenase (GDH, ~ 340,000 Da) using an Agilent 6560 IM-Q-TOF. Collisional cross sections for folded ubiquitin, cytochrome *c*, holo-myoglobin, carbonic anhydrase, human serum albumin (HSA) and GDH were obtained under these conditions and compared with previous DTIM-MS data using this and other instruments. Conditions were also tuned so that nanoESI mass spectra acquired using this DTIM-MS and a TWIM-MS instrument (Waters Synapt G1 HDMS) were comparable in terms of charge state distributions, indicating that similar folded structures were analysed by each method. The stabilities of PLA_2 (PDx) subunits and trimers were demonstrated by comparing drift times of selected ions under a range of cone and trap voltages (DTIM-MS) and solvent conditions (up to 50% methanol, isopropanol and acetonitrile). The broad range of solution and instrument conditions over which these proteins could be analysed, and over which they were stable, largely eliminates the concerns around the choice of experimental parameters to ensure calibrants and analyte proteins are analysed by TWIM-MS and DTIM-MS under the same conditions. CCS of PDx trimer and its β and γ subunits were determined under the optimized native conditions using DTIM-MS to add to the growing database of protein CCS values for calibration of TWIM-MS drift time data. Collisional cross sections of native calibrant proteins (cytochrome *c*, holo-myoglobin, carbonic anhydrase, HSA and haemoglobin) determined by TWIM-MS using PDx monomers and trimer as calibrants were in agreement with the literature values determined directly by DTIM-MS (where available).

These experiments therefore demonstrate optimal conditions for analysis of native-like structures using the Agilent 6560 DTIM-MS and demonstrate the utility of stable calibrants for determination of CCS by TWIM-MS.

Experimental

Materials

MilliQ™ water (Millipore, Bedford, USA) was used in all experiments. Ammonium acetate and methanol were purchased from Ajax Finechem (Seven Hills, Australia). Lyophilized inland taipan (*O. microlepidotus*) venom was purchased from Venom Supplies Pty Ltd. (Tanunda, South Australia). The multimeric PLA_2 paradoxin (PDx) was purified using previously described methods [30, 31] resulting in protein in 200 mM ammonium acetate. Equine heart cytochrome *c*, equine heart myoglobin, HSA, bovine erythrocyte carbonic anhydrase, human haemoglobin, bovine liver GDH (Roche) and bovine erythrocyte ubiquitin were purchased from Sigma-Aldrich (St. Louis, USA).

NanoESI-TWIM-MS and nanoESI-DTIM-MS

All proteins (5–10 μM) were dissolved in 200 mM ammonium acetate and their concentrations determined by measuring the UV absorbance at 280 nm using a ThermoFisher NanoDrop™ 2000c spectrophotometer (Waltham, USA). Glutamate dehydrogenase was passed through a Superdex 200 gel filtration column equilibrated with 200 mM ammonium acetate to ensure buffer exchange. Molar extinction coefficients for the subunits of paradoxin (PDx) were calculated using the ExPASy ProtParam tool and the sequences from the closely related α, β and γ subunits of taipoxin phospholipase A_2 (P00614, P00615 and P00616, respectively.)

NanoESI-DTIM mass spectra were acquired using an Agilent 6560 IM-Q-TOF LC/MS (California, USA) equipped with MassHunter Workstation software and fitted with a nanospray source. The effective length of the drift tube was 1 m. The instrument was fitted with a drift gas upgrade kit holding the drift tube pressure set point within ± 5 mTorr (6.7 μbar) [32]. Samples (2 μL) were nanosprayed from platinum-coated borosilicate capillaries (prepared in-house).

The capillary housing was adapted from the standard nanospray source by fitting of a gas line connected to a N_2 gas supply, enabling application of a low pressure gas flow to help initiate and maintain nanoflow of aqueous samples. The capillary and fragmentor voltages were set to 1.5 kV and 50 V, respectively. The drying gas was left at room temperature with a flow rate of 1.5 L/min. Representative spectra were obtained by summation of 30 s of data acquisition at a given IM entrance voltage for each protein. The resulting spectra were baseline subtracted and smoothed using the Gaussian method in UniDec [33]. Mass calibration was performed prior to data acquisition using Agilent tune mix. Instrument parameters were tuned to obtain nanoESI mass spectra that were consistent with folded, native structures as evidenced by a narrow charge state distribution at relatively high *m/z* (low number of charges). These optimized conditions for native ESI-MS using the Agilent 6560-Q-TOF are shown in Table 1.

NanoESI-TWIM mass spectra were acquired using a Waters Synapt G1 HDMS (Manchester, UK). Samples (2 μL) were nanosprayed from gold-coated borosilicate nanoESI capillaries (prepared in-house). The capillary, sampling cone and extraction cone voltages were set to 1.5 kV, 20 V and 2.0 V, respectively, with the exception of the PDx trimer where the sampling cone voltage was 120 V. The native GDH mass spectrum was acquired with the trap pressure set to 3.6×10^{-2} mbar and collision energies for the trap and transfer were both set to 10 V with a trap bias of 10 V. The trap pressure for all other proteins was set to 3.0×10^{-2} mbar and the IMS gas chamber pressure (N_2) was set to 5.0×10^{-1} mbar. Collision energies for the trap and transfer were to 6 and 4 V, respectively, with a trap bias of 22.5 V for all proteins except GDH (20 V). DriftScope 2.7 was used to visualize a 2D map of drift time (ms) vs *m/z* for the resulting drift plots. This instrument was calibrated for mass using 10 mg/mL CsI. CIUSuite was used to compare the stabilities of proteins against collision-induced unfolding (CIU) as a function of trap voltage and cone voltage and to calculate root-mean squared deviation (RSD) [34].

Determination of Collisional Cross Sections

CCS measurements by DTIM-MS (Agilent 6560 IM-Q-TOF) were achieved using a multifield approach at IM entrance voltages of 1200, 1300, 1400, 1500, 1600 and 1700 V with a drift cell pressure of 3.95 Torr (5.27 mbar) (N_2). CCS calculation was performed using in-built tools in the Agilent IM-MS Browser (B.07.01) software. For the TWIM-MS (Waters Synapt G1 HDMS) CCS determinations, the drift times of the PLA_2 subunit and trimer ions were used to generate calibration curves as previously described [19]. Drift times for each protein ions were

Table 1. Default and Optimized Parameters for All Native Mass Spectra Acquired Using the Agilent 6560 Ion Mobility Q-TOF Mass Spectrometer

Category	Name	Value (default)	Value (optimized)	Unit
IM drift tube	Entrance voltage	1700	1200–1700	Volts
	Exit voltage	250	250	Volts
	Pressure	3.95	3.95	Torr
	Temperature	31	31	°C
	Gas used	N_2	N_2	N/A
IM front funnel	High pressure funnel delta[a]	150	100	Volts
	High pressure funnel RF[a]	200	100	Volts
	Trap funnel delta	180	180	Volts
	Trap funnel exit[a]	10	50	Volts
	Trap funnel RF[a]	200	100	Volts
IM rear funnel	IM hex entrance	41	41	Volts
	IM hex delta	8	8	Volts
	IM hex RF	600	600	Volts
	Rear funnel entrance	200	200	Volts
	Rear funnel exit	35	35	Volts
	Rear funnel RF	130	130	Volts
IM trap	Trap fill time[a]	1000	10,000	μs
	Trap release time[a]	150	2000	μs
	Trap entrance	91	91	Volts
	Trap entrance grid delta	10.2	10.2	Volts
	Trap entrance grid low	99	99	Volts
	Trap exit	90	90	Volts
	Trap exit grid 1 delta	4	4	Volts
	Trap exit grid 1 low	87.8	87.8	Volts
	Trap exit grid 2 delta	8.2	8.2	Volts
	Trap exit grid 2 low	86.6	86.6	Volts
Source	Fragmentor	400	50	Volts
	Gas temp[a]	325	Off	°C
	Flow rate[a]	5.0	1.5	L/min
	Vcap	1700	1500	Volts

[a]Parameters which had the most influence on obtaining native ESI mass spectra

measured with an IM wave velocity of 380 m/s at wave heights of 10.5, 11.0 and 11.5 V.

Results and Discussion

The DTIM-MS (Agilent 6560 IM-Q-TOF) used in this work has been commercially available for several years [18]. A few recent studies have focussed on using this instrument to determine CCS (Ω) for native (folded) biomolecular structures: for example, Gabelica and co-workers [35] noted that RNA and DNA duplexes were compacted in the gas phase compared with canonical solution structures, and recently this group optimized conditions for analysis of ubiquitin and a dimeric quadruplex DNA [36]. McLean and co-workers [37] determined CCS of extended (unfolded, at pH ~ 3) and compact (folded at pH 6.6) ubiquitin, cytochrome *c* and myoglobin. In the current work, solution and instrument conditions were optimized to observe ions in nanoESI mass spectra from native (folded) proteins commonly used as calibrants for ESI-TWIM-MS: ubiquitin (8650 Da), cytochrome *c* (12,360 Da), holomyoglobin (17,560 Da), and also carbonic anhydrase (29,100 Da), HSA (66,472 Da) and GDH (336,510 Da). Table 1 compares the parameters in the default method for protein analysis, with those found best for maintaining folded protein structures. The settings that had the greatest effect on the spectra are noted in the table. Higher capillary voltages (Vcap) and drying gas temperatures led to activation of ions and unfolding of the proteins. The ion count (sensitivity) was increased at lower drying gas flow rates, and high voltages in the high pressure funnel delta and trap funnel RF also decreased ion count for native structures/protein assemblies most likely due to ion heating. Increasing the trap funnel exit voltage and RF peak-to-peak voltage (Vpp) for the octopole ion guide assists larger proteins to the drift cell. Optimization of the trap fill and release times is important to enable a greater accumulation of ions, enhancing sensitivity for larger proteins.

Figure 1 shows mass spectra (acquired using the Agilent 6560 IM-Q-TOF DTIM-MS) of cytochrome *c* using default method settings (Figure 1a) and using the settings optimized here (Figure 1b). The default settings show at least two populations of cytochrome *c*: a folded form which is evident from the abundance of the 7+ ion (*m/z* 1766.4), and a substantially more abundant envelope of ions in which the 12+ ion (*m/z* 1030.9) is most abundant and represents unfolded protein. In contrast, using the conditions applied for analysis of native-like proteins, the 7+ ion is the most abundant in the spectrum in Figure 1b, the 6+ ion is the second most abundant and the 8+ ion is of negligible abundance. This is similar to what was observed by May et al. [37] although in their work the 8+ ion was the second most abundant ion for the folded cytochrome *c* (in 20 mM NH_4OAc), and the 6+ ion was of negligible abundance. This subtle difference is consistent with a greater percentage of folded cytochrome *c* present under the conditions reported here. This charge state distribution is in agreement with that predicted by the Rayleigh limit (Z_R) for cytochrome *c*

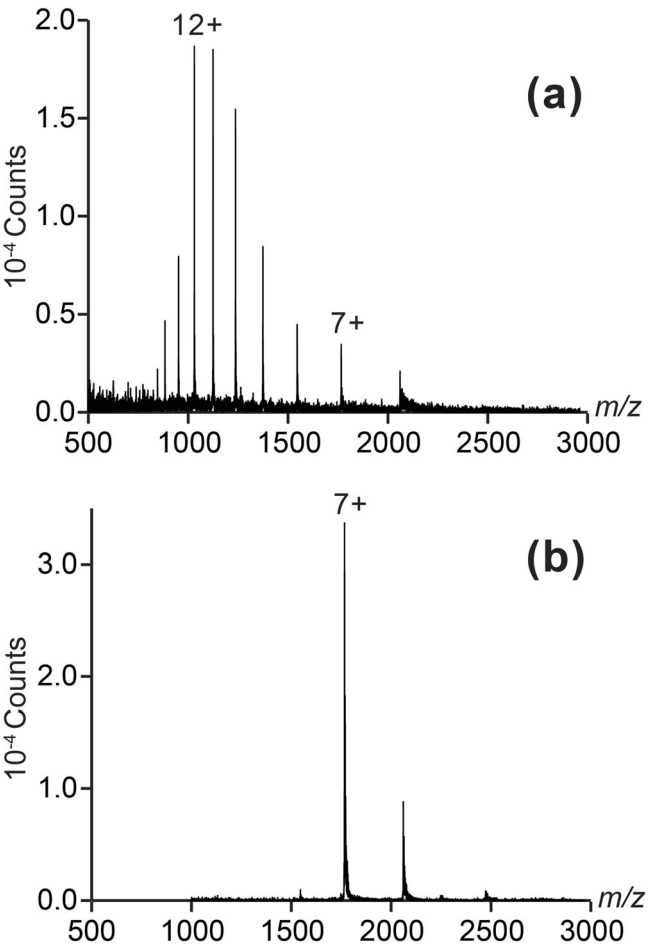

Figure 1. NanoESI mass spectra of cytochrome *c* in 200 mM ammonium acetate acquired using the Agilent 6560 IM-Q-TOF (DTIM-MS). (**a**) Using the default settings (Table 1) with the exception that the trap fill and release times used in (**b**) were applied: 10,000 and 2000 μs, respectively. (**b**) Using optimized settings developed in this work (Table 1)

(8+) supporting that the protein detected is in a globular (folded) form [38].

Since our experiments were first aimed at optimising the DTIM-MS conditions to analyse native proteins and biomolecular complexes, it is important to compare CCS values for ions in the spectra that are likely to arise from folded protein. While good agreement between CCS values has been found between laboratories for biomolecules (e.g. lipids, peptides, proteins, metabolites) [16], comparisons of CCS for native proteins are likely more sensitive to variations in solution conditions, sample handling and mass spectrometry conditions. This is particularly evident in the DTIM mass spectra of ubiquitin (Figure 2a). Under the conditions described in the current work, the 5+ ion was in substantially greater abundance than the 6+ ion in the nanoESI mass spectra. The abundance of the 5+ ion of ubiquitin supports that the protein was substantially in a native-like form. In contrast, in a previous report (Figure 2 of [37]), the 6+ ion was the most abundant, with three collisional cross sections reported for this ion [37]: 1222, 1474 and 1628 $Å^2$. The three CCS represent significant distinct

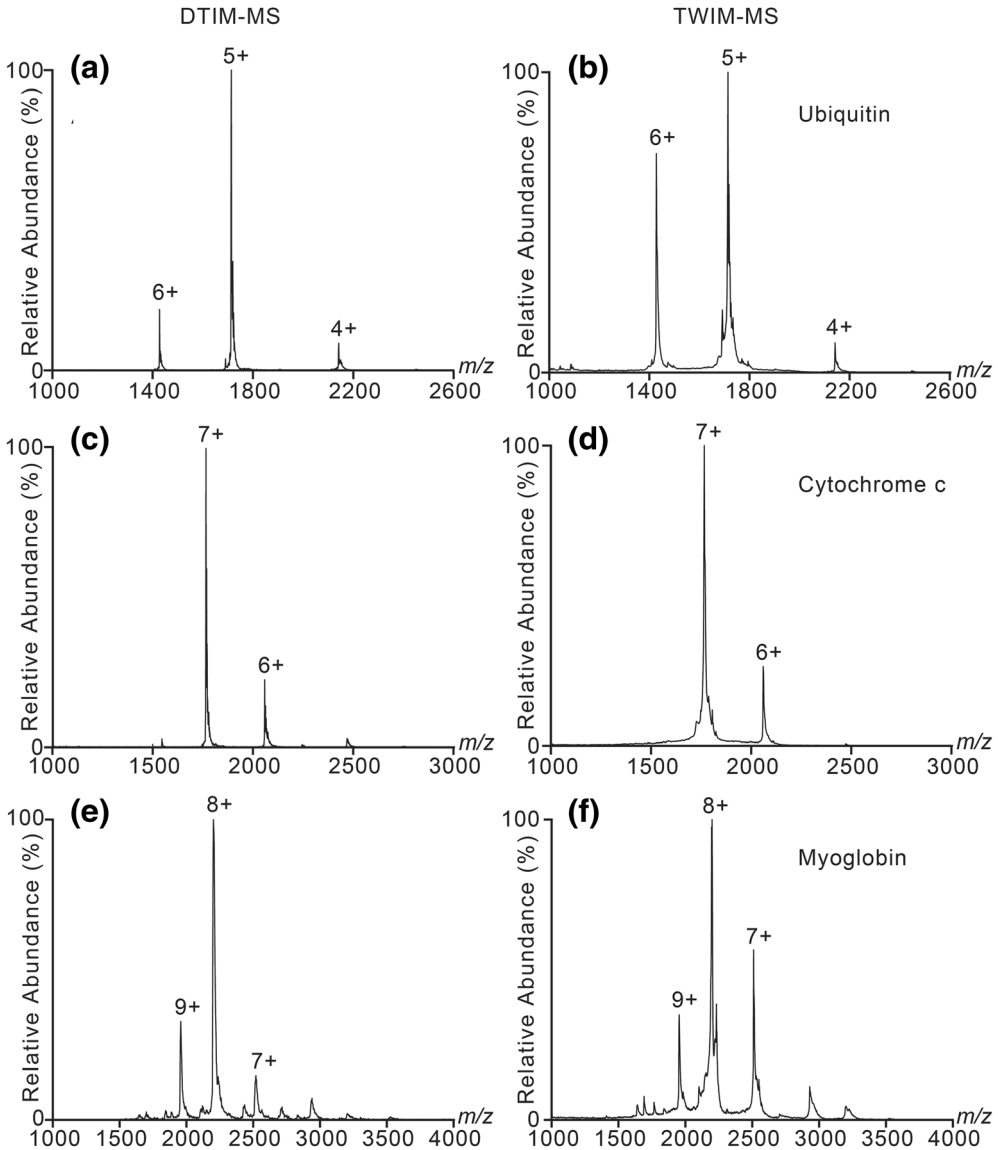

Figure 2. Comparison of nanoESI mass spectra of standard proteins obtained using DTIMS-MS (Agilent 6560 IM-Q-TOF) and TWIM-MS (Waters Synapt G1 HDMS). Ubiquitin: (**a**) DTIM-MS; (**b**) TWIM-MS. Cytochrome *c*: (**c**) DTIM-MS; (**d**) TWIM-MS. Holo-myoglobin: (**e**) DTIM-MS; (**f**) TWIM-MS

conformational forms in the gas phase (and possibly, the 20 mM ammonium acetate solution), with the ions of greater CCS most likely the result of unfolding due to ion heating. Recently, Gabelica et al. [36] also tested tuning parameters for the Agilent 6560 IM-Q-TOF DTIM-MS for analysis of ubiquitin. The 6+ ion was the most abundant in these spectra when they were acquired from solutions of 20 and 50 mM ammonium acetate and 150 mM ammonium acetate, 0.5% sulfolane. Their tuning parameters differed from those presented in the current work, with the most significant differences being the drying gas temperature at 220 °C compared with room temperature (current work), the trap funnel exit at 10 V compared with 50 V (current work) and the trap release time was 200 μs compared with 2000 μs. The longer trap release time was required to accumulate sufficient ions for analysis for larger proteins. It should be noted that longer acquisitions, trap fill and release times significantly increase the ion count for GDH, and may be necessary for analysis of large, multisubunit proteins.

One of the goals of this work was to compare CCS values determined by DTIM-MS and TWIM-MS. Conditions on the TWIM-MS instrument were tuned to produce mass spectra that most closely resembled those observed after DTIMS-MS optimization for native-like protein spectra. Figure 2 compares the nanoESI mass spectra obtained using each instrument for the common calibrant proteins, ubiquitin, cytochrome *c* and holo-myoglobin. The spectra for carbonic anhydrase, HSA and glutamate dehydrogenase are shown in Supplementary Fig. S1. For ubiquitin, cytochrome *c* and holo-myoglobin, the same charge states were the most abundant in the spectra from each

instrument (5+ for ubiquitin, 7+ for cytochrome *c* and 8+ for myoglobin). The similarity in charge state distributions recorded by the two instruments is indicative of similarly folded protein samples in ion sources under both analytical conditions to ensure, as much as is possible, that similar relative populations of accessible conformers exist in both instruments. This is important as a starting point for measurement of CCS from DTIM-MS for the commonly used calibrant proteins (or any proteins) and comparing these with their CCS determined from TWIM-MS. In most of the spectra shown in Figure 2 and Supp. Fig. S1, the spectra obtained using the DTIM-MS showed a slightly greater average charge; for example, in the case of HSA the 16+ ion was most abundant in the spectrum acquired using the DTIM-MS (Supp. Fig. S1 C) while for TWIM-MS (Supp. Fig. S1 D) the 15+ and 16+ ions were of approximately equal abundance. For glutamate dehydrogenase, the DTIM-MS (Supp. Fig. S1 E) favoured the 41+ ion, while in TWIM-MS the 37+ ion was in greater abundance (Supp. Fig. S1 F). The only exception to this was for ubiquitin in which the 6+ ion was of substantially greater abundance in TWIM mass spectra (Figure 2b) than in the DTIM mass spectra (Figure 2a); nevertheless the 5+ ion was in greatest abundance for both instruments.

Table 2 compares CCS values for ubiquitin, cytochrome *c* and holo-myoglobin determined in this work by DTIM-MS (with nitrogen as drift gas) under native-like conditions with analogous DTIM-MS CCS values reported in the literature [11, 37]. In the table, the most abundant ions in the mass spectra are in bold font. Ions at higher *m/z* and lower CCS are more likely to arise from native-like conformations. Comparison of CCS values for the most abundant (native-like) conformer (high *m/z* ions) observed in the DTIM mass spectra in this work, with those for the most abundant conformer of the same charge state reported by May et al. [37], shows reasonable agreement: 1196 (this work, one dominant conformer) compared with 1222 ([37]) for ubiquitin (2.1% difference), 1508 and 1536 for cytochrome *c* (1.9% difference) and 1953 and 1937 for holo-myoglobin (0.8% difference). The results by Bush et al. [11], who used a commercial Synapt HDMS instrument in which the drift cell was replaced by a drift cell with RF ion confinement,

Table 2. Comparison of literature CCS values with CCS values measured under optimized native conditions using DTIM-MS and TWIM-MS (nitrogen as the drift gas)

Protein	z	CCS (Å^2) Literature, DTIM-MS	CCS (Å^2) This work, DTIM-MS	CCS (Å^2) Literature, TWIM-MS	CCS (Å^2) This work, TWIM-MS[a]
Ubiquitin	4	949 (2.2) [37] 1116 (1.4) [37]	967 (1.6) 1116 (1.1)	-	-
	5	1011 (1.7) [37] 1221 (1.9) [37]	**1139 (0.9)**	-	-
	6	**1222 (1.2)** [37] **1474 (1.2)** [37] **1628 (0.8)** [37]	1196 (1.7)	986 [24]	-
Cytochrome *c*	6	1360 (0.9) [37] 1477 (0.4) [37] 1490 [11]	1330 (1.3) 1449 (1.8)	-	1398 (0.5)
	7	**1536 (1.3)** [37] **1590** [11]	**1508 (0.9)**	-	**1533 (0.8)**
Holo-myoglobin	7	1863 (1.7) [37] 1697 (1.7) [37]	1908 (0.9) 1709 (1.6)	-	1788 (0.5)
	8	1937 (1.6) [37]	**1953 (1.0)**	-	**1839 (1.8)**
	9	**2085 (1.8)** [37]	2038 (1.0)	1782 [24]	2010 (0.9)
Carbonic anhydrase	9	-	2520 (1.1) 2309 (1.1)	2004 (0.4) [20]	2425 (0.5)
	10	-	**2580 (1.4)**	2003 (0.8) [20]	**2491 (0.8)**
	11	-	2615 (1.2)	2049 (1.1) [20]	2558 (0.9)
Serum albumin (human, this work; bovine, literature)	14	4490 [11]	4467 (2.2)	-	4521 (0.8)
	15	4490 [11]	4404 (1.5)	-	**4508 (1.0)**
	16	4470 [11]	**4521 (1.9)**	-	**4494 (1.2)**
	17	4490 [11]	4576 (1.8)	-	4531 (1.2)
Hemoglobin	14	-	-	-	4237 (1.2)
	15	-	-	-	4289 (1.6)
	16	-	-	3615 [39]	**4351 (0.1)**
	17	-	-	**3759** [39]	4467 (0.6)
	18	-	-	4552 [24]	4549 (1.7)
Glutamate dehydrogenase	39	13400 [11]	12614 (1.8)	~12400 [43]	-
	40	13400 [11]	12781 (1.3)		-
	41	13500 [11]	**12673 (2.0)**		-
	42		12745 (2.3)		-
	43		12865 (1.0)		-

[a]PDx and it subunits were used as calibrants. The %RSD is given in brackets next to the CCS measurement from this work (for TWIM-MS, from one nanospray needle for each protein at 3 wave heights; for DTIM-MS, 6 nanospray needles (spectra acquired on different days) and 6 IM entrance voltages and where reported directly as %RSD in the literature. Numbers in **bold** show the most abundant ion in the ESI mass spectra (this work and where available from the literature). References to literature CCS are given in superscript

for mammalian serum albumin (bovine in [11], 66,432 Da; human in this work, 66,472 Da) and glutamate dehydrogenase are also in agreement with the CCS reported here: 4521 and 4470 (this work and reported in nm^2 in [11], respectively, 1.1% difference) for serum albumin, and 12,673 and 13,400 (this work and reported in nm^2 in [11], respectively, 5.4% difference) for glutamate dehydrogenase.

In CCS determinations from TWIM-MS experiments, different conditions must be applied to a protein analyte to optimize transmission and resolution (e.g. different wave heights used to separate ions through the travelling wave drift cell [19]). Furthermore, conditions for ionization and IMMS analyses may variably affect the stabilities of common protein standards and the analyte protein(s); hence, the calibrants and the analyte may exhibit different relative populations of varying conformational forms, complicating analyses through overlapping drift times and lower sensitivity, and confounding solution-relevant results. For example, some large proteins/protein complexes require higher cone and trap voltages to increase sensitivity (transmission from the ionization source and through the instrument). In the current work, we tested the very stable PDx trimer and its subunits as calibrants for TWIM-MS CCS measurements.

Figure 3 shows a comparison of the DTIM- and TWIM mass spectra of the snake venom proteins PLA_2, PDx. Both spectra (Figure 3a DTIM-MS and Figure 3b TWIM-MS) reveal ions from the trimer (PDx; ions labelled with charge states only), its γ subunit (ions labelled 'γ') and a small amount of β subunit (ions labelled 'β'). This is consistent with previous studies where the PDx dissociates to a small extent in the mass spectrometer, albeit at higher cone and trap voltages than those applied here [30]. It should be noted that the response factor (most likely the ionization efficiency) for the individual β and γ subunits is substantially greater than for the α subunit and the trimer. Ions from trimer were relatively more abundant when spectra were acquired using the TWIM-MS than the DTIM-MS. In addition, some ions from contaminant proteins (unlabelled peaks in Figure 3) were present in the spectrum acquired using TWIM-MS. The contaminants were not observed by SDS-polyacrylamide electrophoresis. These observations are consistent with contaminants that are of low abundance in solution being more readily ionized and/or transmitted through IMMS than PDx.

The stability of PDx and its subunits was demonstrated by constructing stability heat map plots (Figure 4, drift time against trap and cone voltages in TWIM-MS) for holomyoglobin (8+ ion), the β subunit of PDx (6+ ion) and the PDx trimer (12+ ion). The drift time for myoglobin increases over trap voltages of 20–30 V and a cone voltage of 80–100 V, consistent with unfolding generating more extended conformations; the drift times for the β and γ (latter not shown) subunits of PDx and the PDx trimer were stable over the voltage ranges. The abundance of the PDx trimer was very low at trap voltages greater than 80 V; hence, it was not possible to test its stability at voltages greater than this. The response factor for the α subunit was low under all conditions tested, so it was not tested as a possible calibrant. Supplementary Fig. S2 shows that the PDx proteins were stable over a range of solvent conditions: up to at least 50% acetonitrile, isopropanol and methanol. The high stability of the PDx proteins makes them suitable as stable calibrants across a wide range of solvent and mass spectrometry conditions. Supplementary Figs. S3 and S4 show stability heat map plots and the RSD for variation in drift times as cone and trap voltages, respectively, are increased for the 7+ ion of the β subunit, the 8+ ion of the γ subunit and the 12+, 13+ and 14+ ions of PDx (drift time against cone and trap voltages, respectively). These plots confirm the stability of PDx. The greater variation at shorter drift times (right hand panels) for the trimer most likely reflects dissociation of subunits and/or fragmentation of carbohydrate moieties from the protein. Variation in the heat maps for the 13+ and 14+ ions of PDx likely arises from overlap with ions from αγ complex that is a product of dissociation at higher voltages.

CCS values measured by DTIM-MS (Agilent 6560 IM-Q-TOF) for PDx and its β and γ subunits are shown in Table 3. The stability of PDx is illustrated by the CCS distributions

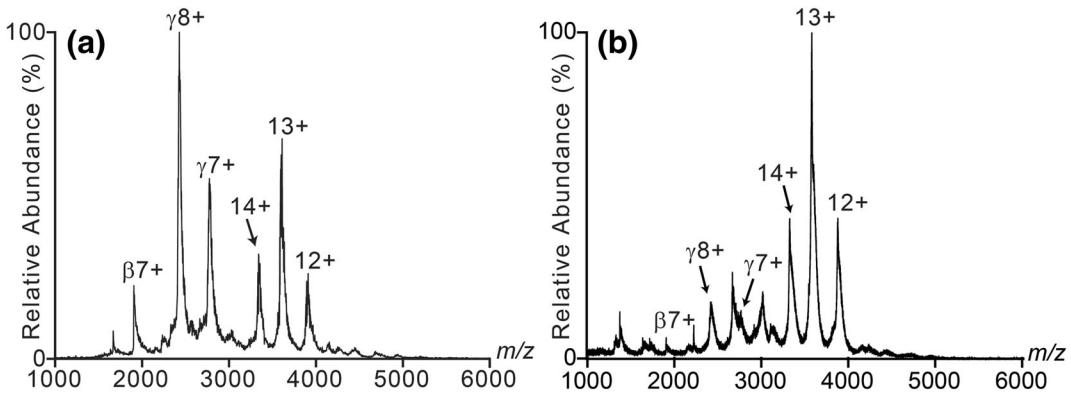

Figure 3. NanoESI mass spectra of the phospholipase A_2, PDx. (**a**) Using DTIMS-MS (Agilent 6560 IM-Q-TOF). (**b**) Using TWIM-MS (Waters Synapt G1). Ions labelled with charge states only are from trimeric PD_x (containing α, β and γ subunits). Ions labelled with charge states and subunit names γ and β are from monomers; ions from contaminant proteins are unlabelled. The contaminant proteins are not sufficiently abundant to be visualized on a SDS-PAGE gel, but ionize and are transmitted highly efficiently in the mass spectrometer; they can be removed by purification of venom using an additional ion exchange step

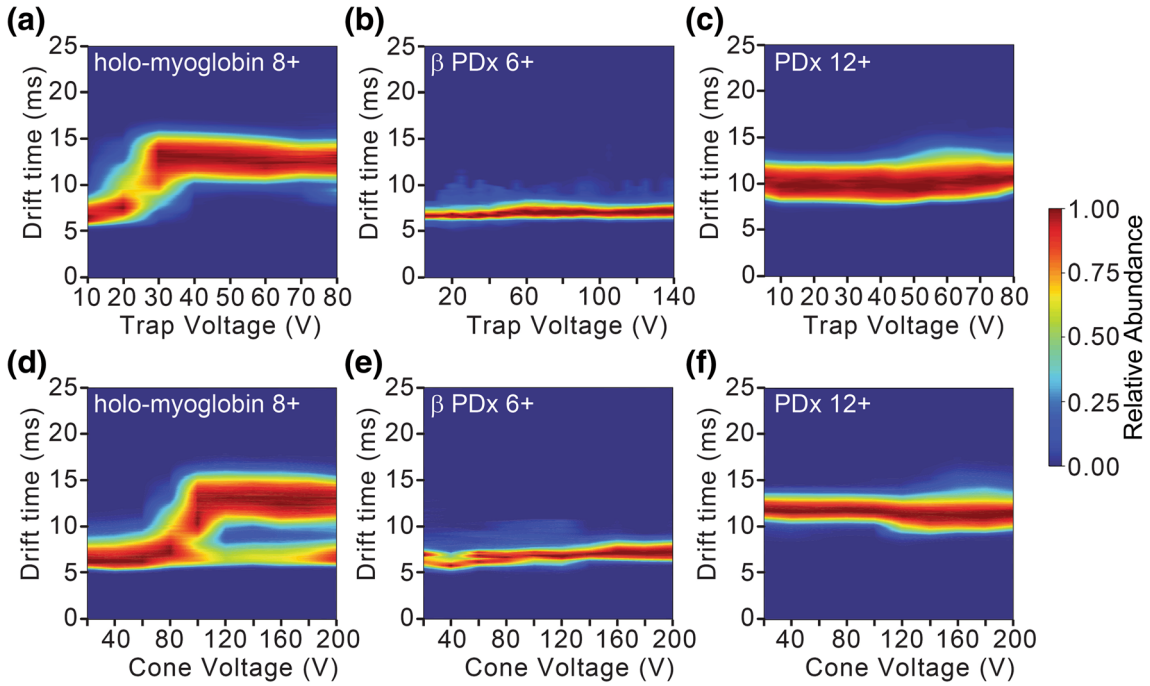

Figure 4. Stability heat maps of proteins as a function of trap and cone voltages (TWIM-MS; Synapt G1 HDMS). Trap voltage: (**a**) Holo-myoglobin (8+); (**b**) β subunit of PDx (6+ ion); (**c**) PDx trimer (12+ ion). Cone voltage: (**d**) Holo-myoglobin (8+); (**e**) β subunit of PDx (6+ ion); (**f**) PDx trimer (12+ ion)

shown in Figure 5 for the 7+ ion of the β subunit, the 8+ ion of the γ subunit and the 12+, 13+ and 14+ ions of PDx, using DTIM-MS and TWIM-MS. Arrival time distributions were converted to CCS using the method of Marchand et al. [41]. The arrival time distributions for these proteins are relatively narrow for DTIM-MS and, notably, also for TWIM-MS compared to the greater difference in drift time resolution (broader arrival time distributions for the TWIM-MS than for DTIM-MS) observed between the two instruments for the common calibrant proteins which are shown in Supp. Fig. S5A, B. The broadening and skewing of arrival time distributions for calibrant proteins underscores the advantages of using stable proteins which maintain narrow distributions across both types of instrumentation. The relatively narrow drift time distributions for the PDx trimer and subunits assist in selection of drift time to be used in calibration plots.

Table 3. DTIM-MS CCS Values of PD_x Trimer and the β and γ Subunits of PD_x Measured Under Optimized Conditions Using an Agilent 6560 IM-Q-TOF

Protein species	Charge *(m/z)*	Measured CCS (Å^2)
PDx trimer	12 (3895.1)	3372 (0.7)
	13 (3595.5)	3438 (1.1)
	14 (3338.7)	3466 (1.1)
β Subunit of PDx	6 (2224.0)	1551 (1.2)
	7 (1906.5)	1561 (0.7)
	8 (1668.5)	1607 (0.2)
γ Subunit of PDx	7 (2770.3)	1717 (1.0)
		1815 (0.9)
	8 (2424.2)	1848 (1.0)

The %RSD is given in brackets next to the CCS measurement. %RSD was calculated from six separate nanospray needles (different analysis days), each at six different entrance voltages. The CCS of the 6+ and 8+ charge states of PDx β were measured three times

The CCS values determined by DTIM-MS and presented in Table 3 enabled PDx trimer and its subunits to be used as calibrants to determine CCS values by TWIM-MS for the standard proteins cytochrome *c*, holo-myoglobin, carbonic anhydrase, HSA and haemoglobin. These results are also shown in Table 2 (right hand column). Calibration plots (using PDx and its β and γ subunits as calibrants) at three travelling wave heights (10.5, 11.0 and 11.5 V) are shown in Supp. Fig. S6. There are many CCS values reported in the literature for these proteins (particularly those determined using DTIM-MS). For cytochrome *c*, the CCS (Å^2) for the most abundant ion in the TWIM mass spectra (7+) was 1533; this is in good agreement with the CCS measured by DTIM-MS (1508 Å^2). In the case of holo-myoglobin, the 8+ ion had a CCS of 1839 Å^2 (TWIM-MS) which was lower than that measured by DTIM-MS in this work (1953 Å^2) and lower that that measured in the literature [37] by DTIM-MS (1937 Å^2). This suggests that the holo-myoglobin analysed in the current TWIM-MS experiments remained in a more folded form, or may have been compacted by loss of solvent. Measurements for this ion were repeated using different samples and conditions. This ion consistently deviated from the calibration plot (see Supp. Fig. S6). The CCS of holo-myoglobin varies significantly over 7+, 8+ and 9+ charge states suggesting a significant effect of charge on the stability of this protein, likely contributing to variability. In future work, other more stable calibrants will be trialled (see Conclusions).

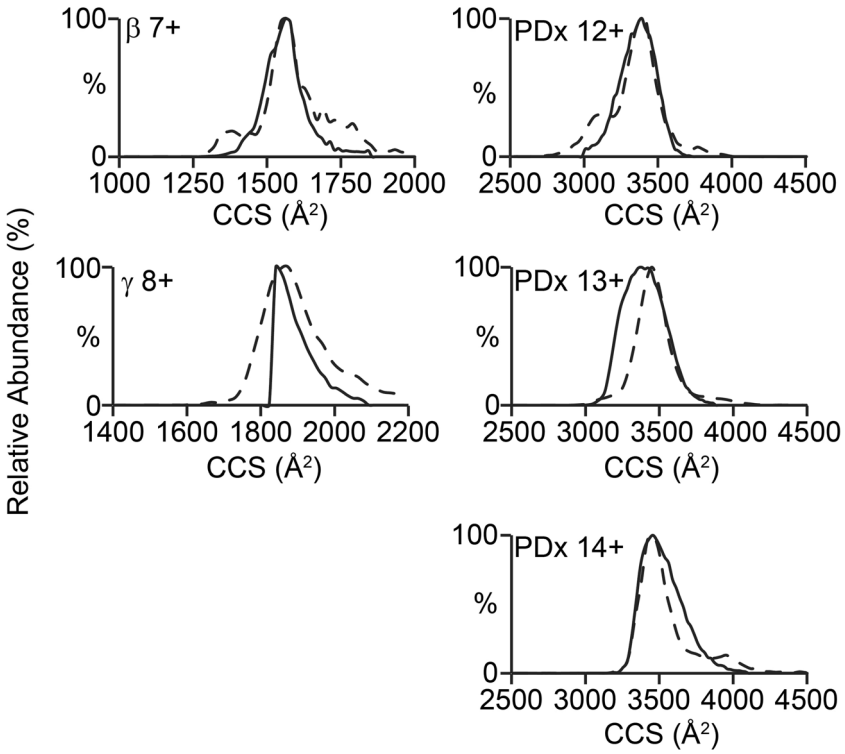

Figure 5. Drift plots (converted to CCS) for the significant charge states observed in DTIM-MS (dashed lines) and TWIM-MS (solid lines) for the 7+ charge state of the β subunit, the 8+ ion of the γ subunit and the 12+, 13+ and 14+ charge states of PDx. For the CCS determined using TWIM-MS, the calibrants were PDx

The agreement between CCS determined by TWIM-MS and DTIM-MS in the present work was reasonable for carbonic anhydrase (2491 and 2580 for the 10+ ion, respectively) and excellent for serum albumin (4494 and 4521 for the 16+ ion, respectively). There are few reliable and consistent determinations of CCS for native-like tetrameric haemoglobin in the literature. Recently, Muralidharan et al. [39] reported TWIM-MS CCS for haemoglobin from fresh hemolysates giving a value for their most abundant 17+ ion of 3759 $Å^2$; this is a smaller cross section than was observed for the 17+ ion in the current work (4467 $Å^2$) and by Konermann and co-workers [24]. This difference may in part reflect the superior spectra obtained from fresh blood samples. This work also used denatured calibrants which may also contribute to this variation.

Overall, the good agreement between the directly measured CCS in DTIM-MS (Agilent 6560 IM-Q-TOF) and the CCS determined by TWIM-MS (Synapt G1 HDMS) using the stable PDx calibrants supports their potential for this application.

Conclusions

Conditions were determined here for MS and IMMS analysis of native proteins using a commercially available DTIM-MS (Agilent 6560 IM-Q-TOF). This DTIM-MS allows for analysis of large proteins and we have demonstrated for the first time acquisition of spectra at the upper *m/z* limit of this instrumentation, with the most abundant ion in the DTIM mass spectrum of glutamate dehydrogenase being the 41+ ion at *m/z* 8202. CCS determined by DTIM-MS under optimized conditions for native-like proteins using nitrogen as the drift gas in this work and by others were in good agreement. The phospholipase A_2, paradoxin (PDx) and its β and γ subunits were very stable with respect to organic solvents and cone and trap voltages in TWIM-MS, and proved to be useful calibrants for determination of CCS using TWIMS: they were stable over a range of conditions and the narrow arrival time distribution allowed for accurate peak selection.

In structural biology, comparison of CCS of folded (native-like) biomolecules can provide insight into conformational switches activated upon ligand binding or dissociation, and about the pathways for assembly and architecture of biomolecular complexes. A limitation of using PDx and its subunits as stable calibrants is that they cover only some of the relevant mass/drift time range relevant to some protein assemblies. In future work, other stable proteins of higher mass will be used to extend the higher mass/longer drift time range to enable CCS determination by TWIM-MS of larger protein assemblies. Snake venoms contain many proteins of higher (and lower) mass than PDx that also exhibit substantial biophysical stability. This is likely a consequence of their proposed evolution from digestive enzymes [42] and their function in nature; they are present in venom glands and must be stable when injected into prey to enable their neurotoxic and myotoxic effects. It is expected that a complete suite of stable proteins for IMMS calibration may be found from this source. Larger stable

proteins from snake venoms are currently being tested in our laboratory. At the other end of the scale, and in addition to venom proteins, small peptide cyclotides will also be tested as calibrants for the lower mass range, high drift time proteins/assemblies.

Acknowledgements

The Waters Synapt G1 HDMS mass spectrometer (University of Wollongong, UOW) used in this work was funded by the Australian Research Council (LE0882289). The Agilent 6560 IM-Q-TOF mass spectrometer (University of Adelaide) was accessed through a collaborative partnership with Agilent Technologies. The work was also supported by Molecular Horizons (UOW).

References

1. Loo, J.A.: Studying noncovalent protein complexes by electrospray ionization mass spectrometry. Mass Spectrom. Rev. **16**, 1–23 (1997)
2. Smith, D.P., Giles, K., Bateman, R.H., Radford, S.E., Ashcroft, A.E.: Monitoring copopulated conformational states during protein folding events using electrospray ionization ion mobility spectrometry mass spectrometry. J. Am. Soc. Mass Spectrom. **18**, 2180–2190 (2007)
3. Porter, K.C., Beck, J.L.: Assessment of the gas phase stability of quadruplex DNA using travelling wave ion mobility mass spectrometry. Int. J. Mass Spectrom. **304**, 195–203 (2011)
4. Eschweiler, J.D., Frank, A.T., Ruotolo, B.T.: Coming to grips with ambiguity: ion mobility mass spectrometry for protein quaternary structure assignment. J. Am. Soc. Mass Spectrom. **28**, 1991–2000 (2017)
5. Wyttenbach, T., Kemper, P.R., Bowers, M.T.: Design of a new electrospray ion mobility mass spectrometer. Int. J. Mass Spectrom. **212**, 13–23 (2001)
6. Harvey, S.R., MacPhee, C.E., Barran, P.E.: Ion mobility mass spectrometry for peptide analysis. Methods. **54**, 454–461 (2011)
7. Lanucara, F., Holman, S.W., Gray, C.J., Eyers, C.E.: The power of ion mobility-mass spectrometry for structural characterization and the study of conformational dynamics. Nat. Chem. **6**, 281–294 (2014)
8. Giles, K., Pringle, S.D., Worthington, K.R., Little, D., Wildgoose, J.L., Bateman, R.H.: Applications of a travelling wave-based radio-frequencyonly stacked ring ion guide. Rapid Commun. Mass Spectrom. **18**, 2401–2414 (2004)
9. Wildgoose, J., McKenna, T., Hughes, C., Giles, K., Pringle, S., Campuzano, I., Langridge, J., Bateman, R.H.: Using a novel travelling wave ion mobility device coupled with a time-of-flight mass spectrometer for the analysis of intact proteins. Mol. Cell. Proteomics. **5**, S14–S14 (2006)
10. Kanu, A.B., Dwivedi, P., Tam, M., Matz, L., Hill, H.H.: Ion mobility mass spectrometry. J. Mass Spectrom. **43**, 1–22 (2008)
11. Bush, M.F., Hall, Z., Giles, K., Hoyes, J., Robinson, C.V., Ruotolo, B.T.: Collision cross sections of proteins and their complexes: a calibration framework and database for gas phase structural biology. Anal. Chem. **82**, 9557–9565 (2010)
12. Williams, J.P., Grabenauer, M., Holland, R.J., Carpenter, C.J., Wormald, M.R., Giles, K., Harvey, D.J., Bateman, R.H., Scrivens, J.H., Bowers, M.T.: Characterization of simple isomeric oligosaccharides and the rapid separation of glycan mixtures by ion mobility mass spectrometry. Int. J. Mass Spectrom. **298**, 119–127 (2010)
13. Clemmer, D.E., Hudgins, R.R., Jarrold, M.F.: Naked protein conformations—cytochrome c in the gas phase. J. Am. Chem. Soc. **117**, 10141–10142 (1995)
14. Shelimov, K.B., Clemmer, D.E., Hudgins, R.R., Jarrold, M.F.: Protein structure in vacuo: gas phase conformations of BPTI and cytochrome c. J. Am. Chem. Soc. **119**, 2240–2248 (1997)
15. Shelimov, K.B., Jarrold, M.F.: Conformations, unfolding, and refolding of apomyoglobin in vacuum: an activation barrier for gas-phase protein folding. J. Am. Chem. Soc. **119**, 2987–2994 (1997)
16. Stow, S.M., Causon, T.J., Zheng, X.Y., Kurulugama, R.T., Mairinger, T., May, J.C., Rennie, E.E., Baker, E.S., Smith, R.D., McLean, J.A., Hann, S., Fjeldsted, J.C.: An interlaboratory evaluation of drift tube ion mobility mass spectrometry collision cross section measurements. Anal. Chem. **89**, 9048–9055 (2017)
17. Smith, D.P., Knapman, T.W., Campuzano, I., Malham, R.W., Berryman, J.T., Radford, S.E., Ashcroft, A.E.: Deciphering drift time measurements from travelling wave ion mobility spectrometry mass spectrometry studies. Eur. J. Mass Spectrom. **15**, 113–130 (2009)
18. May, J.C., Goodwin, C.R., Lareau, N.M., Leaptrot, K.L., Morris, C.B., Kurulugama, R.T., Mordehai, A., Klein, C., Barry, W., Darland, E., Overney, G., Imatani, K., Stafford, G.C., Fjeldsted, J.C., McLean, J.A.: Conformational ordering of biomolecules in the gas phase: nitrogen collision cross sections measured on a prototype high resolution drift tube ion mobility mass spectrometer. Anal. Chem. **86**, 2107–2116 (2014)
19. Ruotolo, B.T., Benesch, J.L.P., Sandercock, A.M., Hyung, S.J., Robinson, C.V.: Ion mobility mass spectrometry analysis of large protein complexes. Nat. Protoc. **3**, 1139–1152 (2008)
20. Leary, J.A., Schenauer, M.R., Stefanescu, R., Andaya, A., Ruotolo, B.T., Robinson, C.V., Thalassinos, K., Scrivens, J.H., Sokabe, M., Hershey, J.W.B.: Methodology for measuring conformation of solvent-disrupted protein subunits using T-WAVE ion mobility MS: an investigation into eukaryotic initiation factors. J. Am. Soc. Mass Spectrom. **20**, 1699–1706 (2009)
21. Jurneczko, E., Kalapothakis, J., Campuzano, I.D.G., Morris, M., Barran, P.E.: Effects of drift gas on collision cross sections of a protein standard in linear drift tube and traveling wave ion mobility mass spectrometry. Anal. Chem. **84**, 8524–8531 (2012)
22. Salbo, R., Bush, M.F., Naver, H., Campuzano, I., Robinson, C.V., Pettersson, I., Jorgensen, T.J.D., Haselmann, K.F.: Traveling wave ion mobility mass spectrometry of protein complexes: accurate calibrated collision cross-sections of human insulin oligomers. Rapid Commun. Mass Spectrom. **26**, 1181–1193 (2012)
23. Allison, T.M., Landreh, M., Benesch, J.L.P., Robinson, C.V.: Low charge and reduced mobility of membrane protein complexes has implications for calibration of collision cross section measurements. Anal. Chem. **88**, 5879–5884 (2016)
24. Sun, Y., Vahidi, S., Sowole, M.A., Konermann, L.: Protein structural studies by traveling wave ion mobility spectrometry: a critical look at electrospray sources and calibration issues. J. Am. Soc. Mass Spectrom. **27**, 31–40 (2016)
25. Morsa, D., Gabelica, V., De Pauw, E.: Fragmentation and isomerization due to field heating in traveling wave ion mobility spectrometry. J. Am. Soc. Mass Spectrom. **25**, 1384–1393 (2014)
26. Hines, K.M., May, J.C., McLean, J.A., Xu, L.B.: Evaluation of collision cross section calibrants for structural analysis of lipids by traveling wave ion mobility mass spectrometry. Anal. Chem. **88**, 7329–7336 (2016)
27. Kang, T.S., Georgieva, D., Genov, N., Murakami, M.T., Sinha, M., Kumar, R.P., Kaur, P., Kumar, S., Dey, S., Sharma, S., Vrielink, A., Betzel, C., Takeda, S., Arni, R.K., Singh, T.P., Kini, R.M.: Enzymatic toxins from snake venom: structural characterization and mechanism of catalysis. FEBS J. **278**, 4544–4576 (2011)
28. Singh, R.R., Chang, J.Y.: Investigating conformational stability of bovine pancreatic phospholipase A(2): a novel concept in evaluating the contribution of the 'native framework' of disulphides to the global conformational stability of proteins. Biochem. J. **377**, 685–692 (2004)
29. Burke, J.E., Dennis, E.A.: Phospholipase A(2) structure/function, mechanism, and signaling. J. Lipid Res. **50**, S237–S242 (2009)
30. Harrison, J.A., Aquilina, J.A.: Insights into the subunit arrangement and diversity of paradoxin and taipoxin. Toxicon. **112**, 45–50 (2016)
31. Skejic, J., Hodgson, W.C.: Population divergence in venom bioactivities of elapid snake *Pseudonaja textilis*: role of procoagulant proteins in rapid rodent prey incapacitation. PLoS One. **8**, e63988 (2013)
32. Kurulugama, R.T., Darland, E., Kuhlmann, F., Stafford, G., Fjeldsted, J.: Evaluation of drift gas selection in complex sample analyses using a high performance drift tube ion mobility-QTOF mass spectrometer. Analyst. **14**, 6834–6844 (2015)
33. Marty, M.T., Baldwin, A.J., Marklund, E.G., Hochberg, G.K., Benesch, J.L., Robinson, C.V.: Bayesian deconvolution of mass and ion mobility spectra: from binary interactions to polydisperse ensembles. Anal. Chem. **87**, 4370–4376 (2015)
34. Eschweiler, J.D., Rabuck-Gibbons, J.N., Tian, Y.W., Ruotolo, B.T.: CIUSuite: a quantitative analysis package for collision induced unfolding

measurements of gas phase protein ions. Anal. Chem. **87**, 11516–11522 (2015)
35. Porrini, M., Rosu, F., Rabin, C., Darre, L., Gomez, H., Orozco, M., Gabelica, V.: Compaction of duplex nucleic acids upon native electrospray mass spectrometry. ACS Central Science. **3**, 454–461 (2017)
36. Gabelica, V., Livet, S., Rosu, F.: Optimising native ion mobility Q-TOF in helium and nitrogen for very fragile noncovalent structures. J. Am. Soc. Mass Spectrom. (2018). https://doi.org/10.1007/s13361-018-2029-4
37. May, J.C., Jurneczko, E., Stow, S.M., Kratochvil, I., Kalkhof, S., McLean, J.A.: Conformational landscapes of ubiquitin, cytochrome c, and myoglobin: uniform field ion mobility measurements in helium and nitrogen drift gas. Int. J. Mass Spectrom. **427**, 79–90 (2018)
38. Susa, A.C., Xia, Z.J., Tang, H.Y.H., Tainer, J.A., Williams, E.R.: Charging of proteins in native mass spectrometry. J. Am. Soc. Mass Spectrom. **28**, 332–340 (2017)
39. Muralidharan, M., Das, R., Bhat, V., Mandal, A.K.: Analysis of the quaternary structure of hemoglobin Beckman variant and molecular interpretation of its functional abnormality: a mass spectrometry-based approach. Chembiochem. **19**, 633–640 (2018)
40. Ma, X., Zhou, M.W., Wysocki, V.H.: Surface-induced dissociation yields quaternary substructure of refractory noncovalent phosphorylase B and glutamate dehydrogenase complexes. J. Am. Soc. Mass Spectrom. **25**, 368–379 (2014)
41. Marchand, A., Livet, S., Rosu, F., Gabelica, V.: Drift tube ion mobility: how to reconstruct collision cross section distributions from arrival time distributions? Anal. Chem. **89**, 12674–12681 (2017)
42. Casewell, N.R., Huttley, G.A., Wuester, W.: Dynamic evolution of venom proteins in squamate reptiles. Nat. Commun. **3**, (2012)
43. Samulak, B.M., Niu, S., Andrews, P.C., Ruotolo, B.T.: Ion mobility-mass spectrometry analysis of cross-linked intact multiprotein complexes: enhanced gas phase stabilities and altered dissociation pathways. Anal. Chem. **88**, 5290–5298 (2016)